Composites Part B 208 (2021) 108599

Contents lists available at ScienceDirect

Composites Part B

journal homepage: www.elsevier.com/locate/compositesb

Stress induced carbon fiber orientation for enhanced thermal conductivity of epoxy composites

Maohua Li [a,b,c], Zulfiqar Ali [a], Xianzhe Wei [a], Linhong Li [a,b], Guichen Song [a], Xiao Hou [a], Hainam Do [d], James C. Greer [c,***], Zhongbin Pan [e], Cheng-Te Lin [a,b], Nan Jiang [a,b,**], Jinhong Yu [a,b,*]

[a] Key Laboratory of Marine Materials and Related Technologies, Zhejiang Key Laboratory of Marine Materials and Protective Technologies, Ningbo Institute of Materials Technology and Engineering, Chinese Academy of Sciences, Ningbo, 315201, China
[b] Center of Materials Science and Optoelectronics Engineering, University of Chinese Academy of Sciences, Beijing, 100049, China
[c] University of Nottingham Ningbo New Materials Institute, Department of Electrical and Electronic Engineering, University of Nottingham Ningbo China, 199 Taikang East Road, Ningbo, 315100, China
[d] Department of Chemical and Environmental Engineering, University of Nottingham Ningbo China, 199 Taikang East Road, Ningbo, 315100, China
[e] School of Materials Science and Chemical Engineering, Ningbo University, Ningbo, 315211, China

ARTICLE INFO

Keywords:
Carbon fiber
Thermal conductive composite
Alignment
Mechanical

ABSTRACT

Polymer composites that have high thermal conductivity have become one of the most promising solutions needed to satisfy the thermal management requirements for high-power electrical and electronic equipment. In this work, a strategy relying on aligning carbon fibers through the application of a stress field is proposed. Ultrahigh through-plane thermal conductive epoxy composites with carbon fiber networks have been prepared by in-situ solidification within an epoxy. The thermal conductivity of these epoxy composites reaches as high as 32.6 W m^{-1} K^{-1} at 46 wt percent (wt%) of carbon fibers, which is about 171 times that of the pure epoxy. The alignment condition for the carbon fibers for a carbon fiber composite in which stress has been applied and a blended carbon fiber composite are compared using micro compute tomography (micro-CT) and scanning electron microscopy (SEM). These epoxy composites display attractive thermal properties and provide a practical route to satisfy the thermal dissipation requirements raised by the development of modern electrical devices and systems.

1. Introduction

With the continued development of high-performance electrical equipment with increasing power densities, the generation of waste heat has become an inevitable risk leading lower performance and shortened product lifetimes. Since traditional electrical packaging materials are inadequate to satisfy the increased demand to dissipate waste heat during device operation, the design of new thermal conductive materials emerges with increasing importance as new research focus. Epoxies are widely used in the thermal management for electrical equipment due to their compatibility with mass-production manufacturing, low toxicity, and low cost. Hence the use of epoxy has been enhanced to solve the waste heat problem by promoting their thermal transport performance through the use epoxy-based composites [1–7]. Various fillers have been used to construct enhanced thermally conductive composites [8–13]. The thermal conductivity of a composite depends both on the intrinsic thermal conductivity of the host material, interface thermal resistance and the percentage content of the fillers. For one-dimensional fillers specifically, the aspect ratio is also a key factor in achieving high thermal conductivity in a preferred direction.

Aligned carbon fibers (CFs) form a one-dimensional thermal conductive filler whose intrinsic thermal conductivity can reach as high as 900 W m^{-1} K^{-1} along the axial direction whereas in the radial direction the value can be as low as 100 W m^{-1} K^{-1}. Compared with

*** Corresponding author.
** Corresponding author. Center of Materials Science and Optoelectronics Engineering, University of Chinese Academy of Sciences, Beijing, 100049, China.
* Corresponding author. Key Laboratory of Marine Materials and Related Technologies, Zhejiang Key Laboratory of Marine Materials and Protective Technologies, Ningbo Institute of Materials Technology and Engineering, Chinese Academy of Sciences, Ningbo, 315201, China.
E-mail addresses: Jim.Greer@nottingham.edu.cn (J.C. Greer), jiangnan@nimte.ac.cn (N. Jiang), yujinhong@nimte.ac.cn (J. Yu).

https://doi.org/10.1016/j.compositesb.2020.108599
Received 14 October 2020; Received in revised form 18 December 2020; Accepted 22 December 2020
Available online 29 December 2020

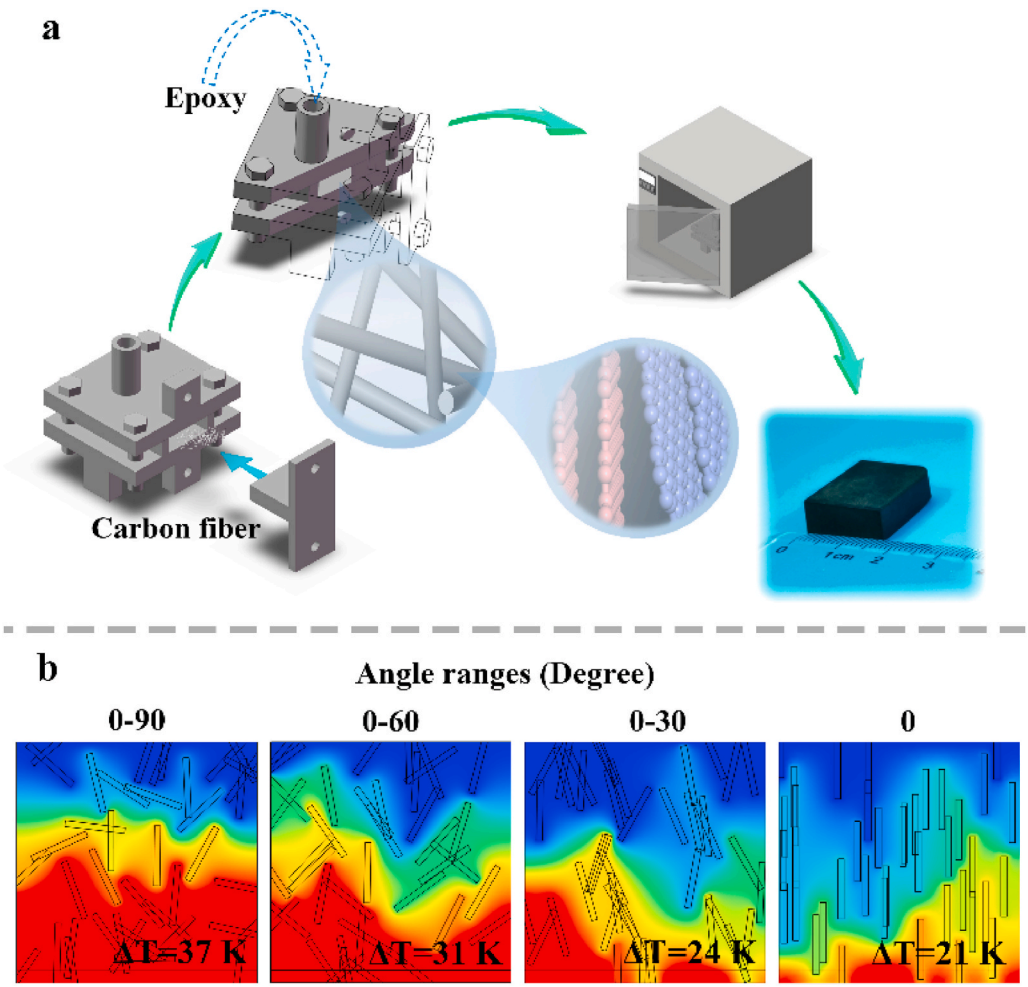

Fig. 1. Schematic illustration of CFs alignment method and simulation. **(a)** the process for aligning CFs by application of stress field. Milled CFs are condensed by mold custom-designed for this purpose. The epoxy is then injected into the mold and solidified at specific temperature. Aligned samples are acquired whose predicted microstructure is shown in the schematic map. **(b)** Temperature distribution calculated by finite element analysis of 1D filler distributed in epoxy with vary alignment conditions. The top surface is fixed at 293.15 K and a 100 W m^{-3} heater is attached to the bottom of block. The temperature difference between top and bottom is labeled which indicates the dependence of thermal conductivity on filler alignment.

metals and ceramics, CF shows a lower mass density but displays comparable mechanical properties. To take advantage of the thermal conductivity properties of CFs different methods have been developed. Among these, common strategy is to use hybrid fillers by adding related materials such as graphene and carbon nanotubes, or to use metal fillers [14–19]. Hybrid fillers can enhance thermal conductivity due to the bridging effect of fillers of different. Heat flow can be passed between CF bundles via these smaller scale fillers as opposed to relying on the heat transfer properties of the matrix. In a relevant study, Yu et al. point out that Cu plated on CF surfaces promotes the thermal conduction selectively for the in-plane direction by more than a factor of three, reaching 7.37 W m^{-1} K^{-1} with a significantly smaller improvement on the through-plane direction [14].

Two alternate approaches to promote thermal conductivity are usage of surface modification and alignment of CFs. By modifying surface of CFs with multilayer covalent grafts, Yu et al. linked bismaleimide, an epoxy initiator, with filler enhancing the binding between the matrix and CFs supporting the transfer of heat in the epoxy to be more efficiently transferred to the filler [20]. The sample showed 125.5% higher thermal conductivity at 1.25 wt% loading. Their simulations reveal that a better bonding or coupling between the filler and matrix results in a more efficient heat transfer from resin to filler. Varshney et al. simulated heat transfer between CF and a matrix using the LAMMPS molecular dynamics simulation package and find a positive correlation between interfacial density of functionalization groups and interface thermal conductance. The thermal conduction increase up to four-fold at a point where the interfacial density of the functionalization groups reaches up to 0.55 molecule nm^{-2} [21].

Surface modification reduces the interfacial thermal resistance between CF and epoxy, while the alignment can take use of the 900 W m^{-1} K^{-1} thermal conductivity along the axial direction better. And compared with surface modification, introducing new chemical is not necessary for aligning CF. Alignment of fillers can be achieved by application of a magnetic field or electronic field, and the use of templates and melt extrusion [22–31]. Using nickel as an additive to assist the orientation of CFs in a magnetic field, Ren et al. achieved a 90% enhancement in thermal conductivity [23] as the nickel particles plated onto the CFs endow the filler with magnetic responsiveness. This enables controllable thermal properties by adjusting the applied magnetic field. Another important work demonstrating the alignment of CFs was undertaken by Uetani et al. [22] In their work, electrostatic flocking was used to align CFs wit a through-plane orientation. A three-dimensional neat of aligned CFs is observed and results in an outstanding thermal conductivity result of 23.3 W m^{-1} K^{-1}, at ~13 wt% CF. However, the ~30 kV voltage which is energy-consuming and unsafe used in this work is a direction to promote. Recently Ma et al. applied the use of an ice template to align CFs [26]. During the growth of the template, the formation of vertically oriented ice crystals promotes the alignment of the CFs to be along the through-plane direction. After freeze-drying, three-dimensional (3D) CF networks are obtained. With this technique, the authors report a thermal conductivity of 2.84 W m^{-1} K^{-1} at 13 vol% filler loading. By applying strong shear and extension flow field during extrusion, Zhang et al. constructed high orientation and ordered distribution and achieved 2.05 W m^{-1} K^{-1} thermal conductivity [31].

Although the field of thermally conductive insulating materials has been developed over several decades, there remain many challenges to

the further improvement in the values of thermal conductivity. Foremost for hybrid filler systems, a generic problem to previous approaches is that CFs cannot be in direct contact. In instances, they are mixed with a resin which breaks the heat path between individual CFs. In other instances, CFs are bridged by a second filler introducing two sources of interfacial thermal resistance between the bridging fillers and CFs. Related to these approaches are concerns for the choice of surface modification, the use of toxic chemicals and time-consuming process are difficult to avoid. After that, for alignment of CFs, it is hard to achieve a high thermal conductivity without a method requiring large power-consumption. Although there are obvious thermal conductivity gains in these reports, it is difficult to achieve a thermal conductivity in excess of 10 W m^{-1} K^{-1} without an electric field with an associated high voltage source.

In this study, CFs framework were formed with a load force creating a stress field in the carbon fibers before injecting resin. In the initial framework, all CFs are supported within a network of the other CFs, which provides a continuous network for thermal conduction. It is hypothesized and will be demonstrated in this work that an alignment between the individual CFs is induced by the application of the stress field. A high value of thermal conductivity of 32.6 W m^{-1} K^{-1} at 46 wt% CFs loading will be demonstrated without the need for techniques that do not require high power or the use of toxic materials. The electrically-insulating thermal conductor materials that are reported are promising solutions to the issues of thermal management of modern high performance electrical equipment.

2. Experimental

2.1. Materials

The epoxy resin and curing agent methylhexahydrophthalic anhydride (MHHPA) were provided by Dow Chemical Company and Zhejiang Alpharm Chemical Technology Co. Ltd., respectively. The curing accelerator Neodymium(III) acetylacetonate trihydrate (Nd(III)acac) was obtained from Sigma-Aldrich Corporation. Carbon fibers were provided by Fujian United New Material Technology Co., Ltd. (Fujian, China) and are used as thermal conductive filler. All other chemicals were of analytical reagent grade and used without further purification.

2.2. Preparation of epoxy composites

Epoxy, curing agent, and accelerator were blending in a ratio of 100:95:0.5, respectively, with a stirring de-aerator. A mold as shown in Fig. 1(a) (for which a photograph can be found in the supplementary material; Fig. S1), was designed to hold the raw materials. 3.5 g of CFs are compressed into the mold with the use of a plug and epoxy is injected. The entire mold is placed into a vacuum oven where the temperature is held fixed at 70 °C to improve the flow properties of the epoxy. The air in mold is pumped out to allow the epoxy to flow into the mold. During this process, the lowering of the liquid level in the bore can be observed. Additional epoxy is added while the air is evacuated until the liquid level does not lower. Curing of epoxy is achieved in an oven where two temperature cycles are set. In the first cycle, the temperature held at 135 °C for 2 h to pre-cure the epoxy. In the second cycle, the temperature is held at 165 °C for 14 h. The concentration of CFs varies from 30 to 46 wt%. These samples are pre-stressed carbon fiber epoxy composites henceforth denoted as s-CF/Epoxy. On the other hand, epoxy, curing agent and CFs are mixed in equal proportions in a single pot and blended using a speed mixer. The curing method follows the same procedure as for the s-CF/Epoxy. The carbon fiber epoxy composites are prepared by blending with the resulting blend denoted as CF/Epoxy. In addition, when preparing CF/Epoxy samples, it was difficult to ensure the raw materials form a homogeneous mixture once the concentration of the CFs exceeds 35 wt%. In these cases, acetone is used to dilute the epoxy resulting in homogeneous samples. For these higher concentrations of CFs. an additional step is introduced to remove the acetone, which is achieved by keeping a sample at 70 °C for 12 h before solidification.

2.3. Characterization

To characterize the carbon fiber, Fourier transform infrared (FTIR) spectra, X-ray diffraction (XRD) patterns, and Raman spectra were obtained using a Nicolet 6700 spectrometer (Thermo Fisher), a Bruker D8 Advanced diffractometer, and a Renishaw Reflex Raman System, respectively. Thermal diffusivity at different temperatures, volumetric heat capacity of composites and concentration of CFs were measured by a laser flash apparatus (LFA; NETZSCH LFA 467), differential scanning calorimetry (DSC; NETZSCH DSC 214), and thermal gravimetric analysis (TGA; NETZSCH TGA209), respectively. The morphologies of the CFs are observed with scanning electron microscopy (SEM; FEI Quanta FEG 250). The mold is custom designed and produced in our laboratory. The alignment of the CFs in the composites are analyzed by micro-computed tomography (micro-CT) using a ZEISS Xradia 510 Versa.

Thermal conductivity is calculated according to:

$$k = \alpha C_p \rho \tag{1}$$

where α, C_p, ρ refer to thermal diffusivity (mm^2 s^{-1}), specific heat (J g^{-1} K^{-1}) and density (g cm^{-3}), respectively. Here, the heat capacity is measured by DSC with sapphire as a reference. Composite samples were heated to 1000 °C at a rate of 10 °C min^{-1} under a nitrogen ambient. Epoxy composites decompose at 450 °C and the residual weight is regarded as weight of the CFs. The infrared images demonstrating temperature difference is taken using an Fluke infrared (IR) camera. The mechanical properties of the composites are evaluated by dynamic mechanical analysis (DMA) using a TA Instruments DMAQ800.

3. Result and discussion

To illustrate the influence on thermal conductivity of aligning the CFs, a Finite Element Analysis was performed. The CFs are modified by 20 continued bars whose length-width ratio is 10 and matrix covering all CFs are modified by a rectangle. A thin heater with a volume power density of 100 W m^{-3} is attached to the bottom of the different composites to set up a heat flux with a gradient in the preferred alignment direction of the CFs. The CFs are distributed quasi-randomly with the ranges of the angle of the CF rod's primary axis with respect to the temperature gradient as specified in Fig. 1(b); note that an angle of zero represents a CF aligned along the direction of the temperature gradient and angle of 90° corresponds to the CF being perpendicular to the temperature gradient. The top-surface temperature of composite is fixed at room temperature which is taken to be 293.15 K and the temperature difference between top-surface and bottom at the equilibrium is labeled as shown in Fig. 1(b). The definition of thermal conductivity is given as

$$k = \frac{Q}{\nabla T S} \tag{2}$$

where Q is the power of heater, S is the cross sectional area of the model, and ∇T is the gradient of temperature. For constant power input and cross sectional area, thermal conductivity is inversely proportional to the thermal gradient ∇T. When the angle range is 0–90°, the direction of carbon fibers is totally random, which results in a zigzagging heat path and thus the heat cannot pass through composite rapidly due to a long path length for heat transfer relative to the length of the sample. The heat is built up in the sample resulting in a temperature increase. Due to the fixed temperature of the cooling area, the end result is a larger temperature difference. On the contrary, with the angle of the CFs with respect to the temperature gradient becomes zero or to say the CFs are fully aligned with the preferred direction of heat transport, the heat path is at a minimum resulting more efficient heat transfer. The temperature

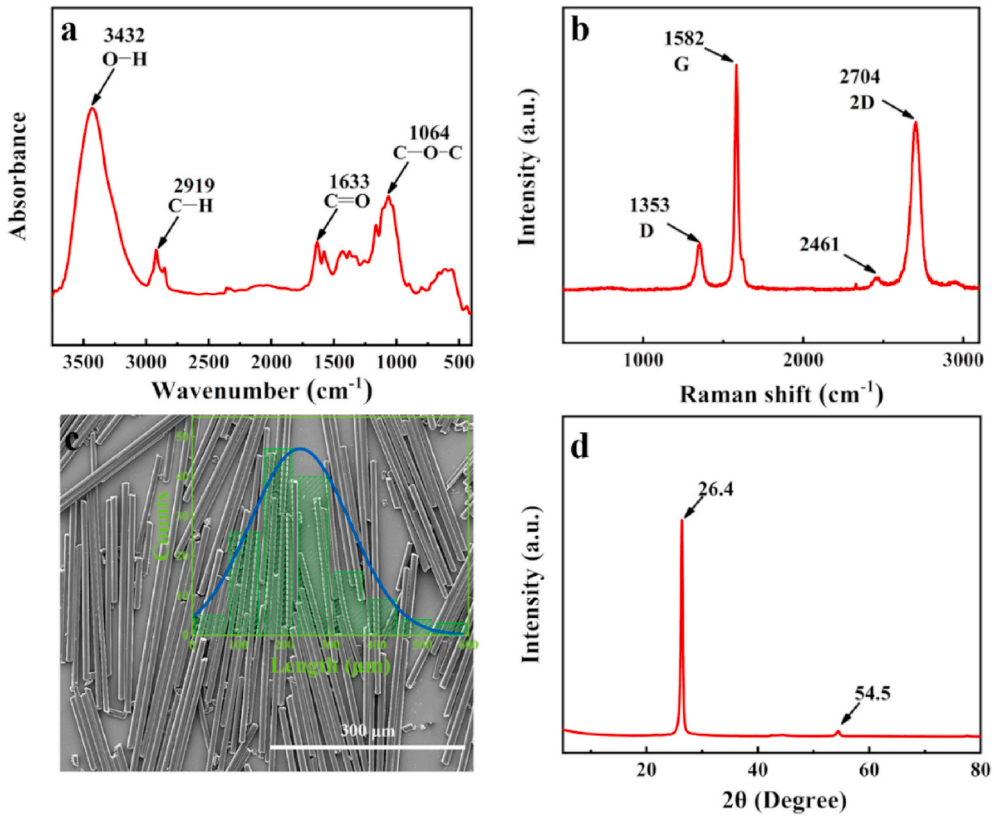

Fig. 2. Characterization of milled CF. **(a)** IR spectrum **(b)** Raman spectrum **(c)** microstructure and statistic of CF length **(d)** XRD spectrum.

differential reduces from 37 to 21 K. In conclusion, the simulation results demonstrate the principle that the alignment of CFs is an efficient method to enhance the thermal conduction in CF composites. To achieve alignment in the experimental studies, a strategy is devised by applying a force to the CF powders. We hypothesize that the alignment of the CFs is achieved during the period of time the force is applied.

FTIR is a sensitive method for detecting functional groups binding to the surface of the carbon fibers. In the observed FTIR spectrum, the peaks at 3443, 2919, 1633 and 1064 cm^{-1} are assigned to stretching mode vibrations of O–H, C–H, C═O, and C–O, respectively. Among them, the O–H bond can be associate to absorbed water on the CF surface [32]. Raman spectroscopy is used to analyze amorphous carbonaceous structures. The Raman spectrum of the milled CF is similar to that of graphene. In the Raman spectrum, bands located at 1353, 1582, 2461 and 2704 cm^{-1} are labeled as D, G, D+D″ and 2D bands. The D-band is derived from the defects and disorder in the carbonaceous structure, and the G-band arises from ordered graphitic structures [33]. The D+D″ band is related to the combination of D phonon and a longitudinal acoustic branch phonon. Analysis of the SEM image allows for a determination of the distribution of the CF lengths by approximating the average length of CFs to be 250 μm. The distribution of the lengths is then given relative to this average and is shown in Fig. 2(c). XRD is a powerful method to analyze the crystalline structure in the composites. From the XRD pattern, peaks at 26.4° and 54.5° are observed and assigned to graphitic (002) and (004) planes. According to Bragg formula, the interlayer spacings d_{002} and d_{004} are 3.38 and 1.68 Å, respectively.

To explain the orientation of the CFs, one end of a fiber is fixed at a point taken to be the origin. The orientation of CFs can be converted by determining the distribution of the other end a fiber which will lie on a hemispherical surface as depicted in Fig. 3(a). *A* is defined to be the angle between a carbon fiber and the normal vector to the through-plane. If the distribution is totally random, the probability of finding the end on an infinitesimal ring at *A* angle is $\sin(\alpha)dA$. In Fig. 3(b), where *dA* is set at 1°, the resulting probability versus angle is given by grey curve in Fig. 3(b). The orientation distribution of CFs in s-CF/epoxy and CF/epoxy has been characterized by using micro-CT. Compared to the random distribution, s-CF/epoxy samples result in a higher probability of occurrence at small values of *A* and lower probability at larger values of *A* as can also be seen in Fig. 3(b). The statistical data indicates an alignment of the CFs along the normal direction to the through-plane. On the contrary, the CF/epoxy samples result in lower probabilities at small *A* and higher probabilities at larger *A*, which is possibly caused by gravity. In the supporting information, a video whose every frame is a section parallel to the top surface is shown. In the video in supporting information which compares the two samples, we can see the different alignment between differing samples clearly. Fig. 3(d and e) also present the spatial structure of carbon fibers dispersed in the two samples.

SEM images are also used to analyze the orientation of CFs in two-dimensional (2D) space. By studying the morphology of breaking face, statistics for the orientation of the CFs is obtained. As shown in Fig. 3(f), the fibers in s-CF/epoxy tend to orient along the direction of heat transfer, while the fiber in CF/Epoxy samples tend to disperse randomly as Fig. 3(g) show. Statistics results of both samples are given in Fig. 3(b), α here is the angle between CF direction and heat transfer direction which is through plane direction here. The SEM analysis results in conclusions that are substantiated by the phenomenon observed by the micro-CT measurement. In addition to the orientation preference for the CFs in a sample, SEM is also used to illustrate the microstructure in the composites. At the intersection of CF network, epoxy absents as shown in Fig. 3(h). On the contrary, in CF/Epoxy samples, Fig. 3(i) shows that resin is always found between CFs. Given that a force is applied the CFs before injecting epoxy, it can be understood that CFs assemble a network amongst themselves to enable transferal of the applied force to the network, and it is worthwhile noting here that it is also the CF network that contributes to the improvement in the heat transfer. On the

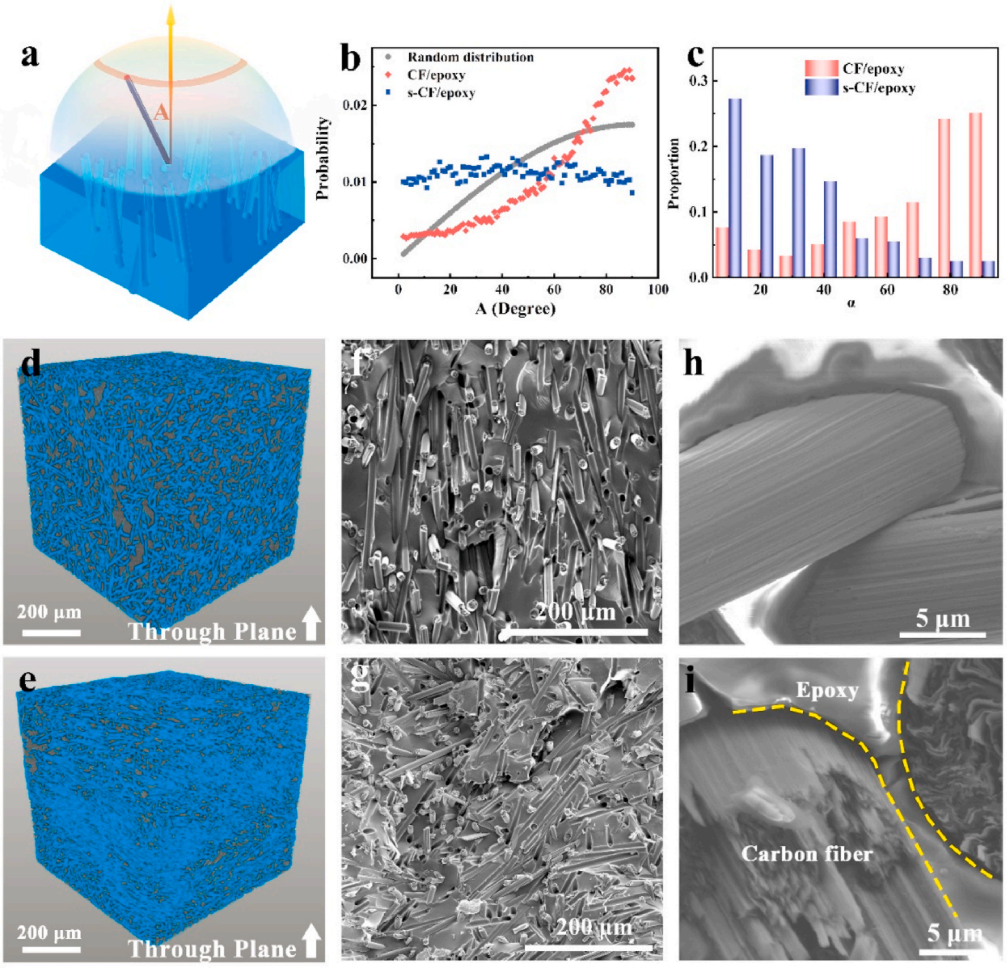

Fig. 3. The characteristic of CFs alignment. **(a)** Schematic of the angle between CFs, denoted A, and the normal vector to the through-plane. **(b)** The statistics of A in CF/epoxy (red dots) and s-CF/epoxy (blue dots) and theoretical value for a purely random distribution (grey dots). **(c)** The statistics of angle between carbon fiber direction and through plane direction according to SEM images. **(d,e)** The micro-CT results of s-CF/epoxy(**c**) and CF/epoxy**(d)**. **(f,g)** The SEM image of composites and statistics of A in s-CF/epoxy**(e)** and CF/epoxy**(f)**. SEM statistics is based on the CF alignment on the 2D cross section, which is different from micro-CT based on that in 3D block **(h,i)** The SEM images showing the direct connection between CFs in s-CF/epoxy**(g)** and the epoxy separating the CFs in CF/epoxy **(h)**. (For interpretation of the references to color in this figure legend, the reader is referred to the Web version of this article.)

contrary, the CFs in control group are cladded by epoxy which introduces additional thermal resistance between CFs, thereby further inhibiting the thermal conduction relative to the aligned CF network.

Fig. 4(a) shows the relationship between thermal conductivity and CF content and provides a comparison between the S-CF/epoxy and CF/epoxy samples. For reference, the result for the pure epoxy is a thermal conductivity of 0.19 W m^{-1} K^{-1}. With the increase of CFs content, the CF/epoxy thermal conductivity improves to 4.7 W m^{-1} K^{-1}. According to our measurement, thermal conductivity is proportional to the loading of CFs and this behavior has been intensively investigated. Agari et al. proposed a model [34] that specially describes the thermal conductivity of composites filled by 1D filler. Within the model, the apparent thermal conductivity is predicted by

$$\log k = VC_2 \log k_f + (1 - V)\log(C_1 k_p) \quad (3)$$

where V is assigned to the volume concentration of fillers. C_1 is factor related to the crystallinity and crystal sizes in the matrix. In this study, the same epoxy as matrix for both s-CF/epoxy and CF/epoxy, so C_1 for the two samples should be equal or nearly so. C_2 is general factor related to the ease of forming conductive chains in the original literature, but the physical meaning of C_2 may be more. The model of Agari et al. takes into consideration the influence of CFs aspect ratio on C_2 but the influence of alignment is not included. The parameters k_f and k_p are the thermal conductivity of filler and matrix, respectively. In the model, a strict restriction that k_f is lower than 418 W m^{-1} K^{-1} (1 cal s^{-1} cm^{-1} $^oC^{-1}$) is implied. However, with the continued developments in material science, many novel fillers have been found whose thermal conductivity is much higher than this limitation, such as the CFs used in this work. In Agari et al.'s model, if k_f is less than 418 W m^{-1} K^{-1}, the higher the likelihood of forming conductive chains, the smaller C_2 becomes. However, in this work, the CFs have a value of 418 W m^{-1} K^{-1} for their thermal conductivity, so the negative sign introduced by $\log k_f$ disappears. As a result, the trend of C_2 should reverse, which means that the more probable it is to form conductive chains, the larger should C_2 becomes. Here, a least square method is used to match the experimental data, during which C_1 is set to the same value for s-CF/epoxy and CF/epoxy composites. According to our calculation, C_1 equals to 7.8. The apparent thermal conductivities calculated according to Agari et al.'s model are shown in Fig. 4(a). The C_2 extracted from the measured data for s-CF/epoxy and CF/epoxy are 6.8 and −0.7, respectively.

From the microstructural characterization, two possible reasons are proposed to explain the difference in the ease of forming conductive chains between s-CF/epoxy and CF/epoxy. Firstly, CFs tend to align along the normal direction to the through-plane under the applied external force. The alignment makes the conductive chains more efficient for heat transport due to the fact that the axial thermal conductivity of the CFs is approximately an order of magnitude higher than that for the radial direction. Another possible reason is that CFs can construct a framework *in situ* to transfer heat in the s-CF/epoxy samples, whereas in the CF/epoxy samples, the epoxy wrapping around CFs break the direct connection between individual CFs. In addition to the SEM analysis based on the images showed in Fig. 3(f) and **(g)**, mechanical property is also investigated to provide support to the conclusions. The epoxy in the composites binds the CFs together. Absence of epoxy between CFs can cause variations to mechanical properties. Previous works have reported the relationship between the damping term (tan δ)

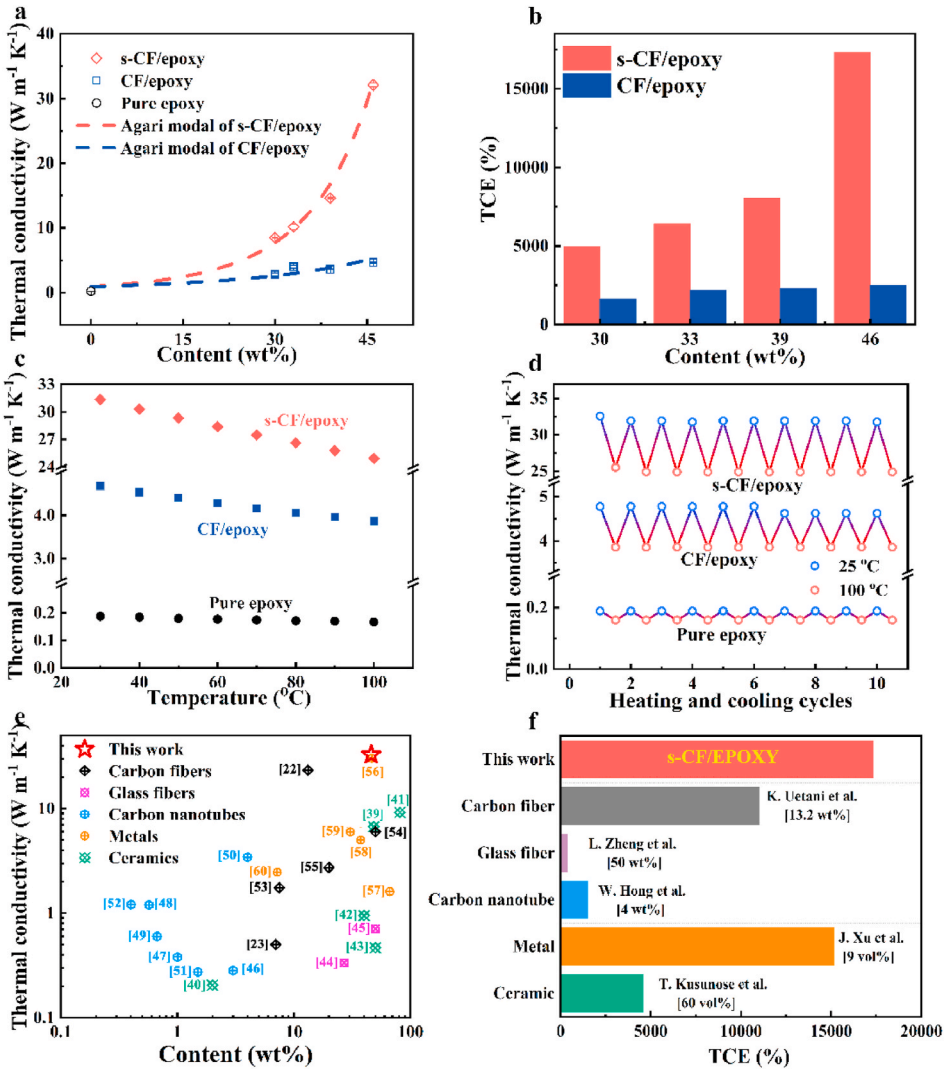

Fig. 4. Thermal conductivity of s-CF/epoxy and CF/epoxy. **(a,b)** Thermal conductivity **(a)** and thermal conductivity enhancement **(b)** as a function of CF concentration in s-CF/epoxy (red) and CF/epoxy (blue). **(c)** The thermal conductivity during 10 heating and cooling cycles. **(d)** The thermal conductivity of s-CF/epoxy, CF/epoxy and pure epoxy at different temperature vary from 30 to 100 °C. **(e)** Comparison of the thermal conductivity and content of the s-CF/epoxy with the thermal conductivity and content of previously reported composites filled by 2D fillers including ceramics (green), glass fibers (purple), carbon nanotubes (blue), CFs (black), metals (orange). (For interpretation of the references to color in this figure legend, the reader is referred to the Web version of this article.)

and interface strength [35–38]. According to the analysis of Ziegel and Romanov, this relationship can be expressed by the following formula:

$$\tan \delta_c = (1 - B\varphi_F)\tan \delta_m \,, \tag{4}$$

where $\tan \delta_c$ and $\tan\delta_m$ are the damping terms of the composite and matrix, respectively, and φ_F is the volume fraction of the filler. B is a correction factor defined to compensate the volume fraction for the interphase resulting from strong interactions at the interfaces in the composite. The value of the parameter B is positively correlated with the interface strength. According to the analysis, the formula demonstrates the decrease of $\tan \delta_c$ with increasing interface strength. In the supplementary material, Fig. S2 shows the DMA results for the s-CF/epoxy, CF/epoxy, and pure epoxy and Fig. S3 shows the strain-stress of s-CF/epoxy and pure epoxy. Relative to the CF/epoxy, the s-CF/epoxy samples have a slightly larger $\tan \delta_c$ which suggests a low concentration or absence of epoxy at the surface of the CFs. The most likely reason for the lower interface strength between epoxy-CF leading to a network of directly connected CFs. This is in agreement with the conclusions for the microstructure as observed by SEM.

Thermal conductivity enhancement (TCE) which is used to characterize the improvement of thermal conductivity of composites compared to a matrix without filler can be calculated according to

$$TCE = \frac{T_C - T_M}{T_M}\ 100\%, \tag{5}$$

where T_C and T_M are the thermal conductivities of the composite and matrix, respectively. Fig. 4(b) compares the TCEs of s-CF/epoxy and CF/epoxy. The best TCE value 17,137% is given by the sample with 46 wt% CFs in s-CF/epoxy. At the same concentration, CF/epoxy gives 2471% enhancement which clearly an improvement over the unfilled matric but is substantially lower than the result for the aligned CFs obtained by prestressing the samples.

Fig. 4(c) illustrates the decrease of thermal conductivity at higher temperatures. When the testing temperature is increased in steps of 10 °C between 30 and 100 °C, the thermal conductivity of the s-CF/epoxy, CF/epoxy, and pure epoxy samples decrease from 32.6, 4.7, 0.19 to 24.9, 3.9 and 0.17 W m^{-1} K^{-1}, which represents percentage drops of 24%, 17% and 11%, respectively. This result indicates that the thermal conductivity decreases as a percentage more rapidly with temperature when the CF content is higher. Fig. 4(d) shows the thermal conductivity during 10 thermal cycles. The thermal conductivity of these three samples are influenced at high temperatures, but can the degradation in thermal conductivity is reversible with the samples returning to pre-thermal stress temperatures after cooling to room temperature. The thermal stability of the composites is a critical consideration for their practical use in electronic applications.

The highest thermal conductivity achieved in this study is 32.6 W m^{-1} K^{-1} at 46 wt%, which is competitive with thermal materials made by using one dimensional (1D) thermal conductive fillers. Fig. 4(e) illustrates the thermal conductivity of composites made with 1D filler

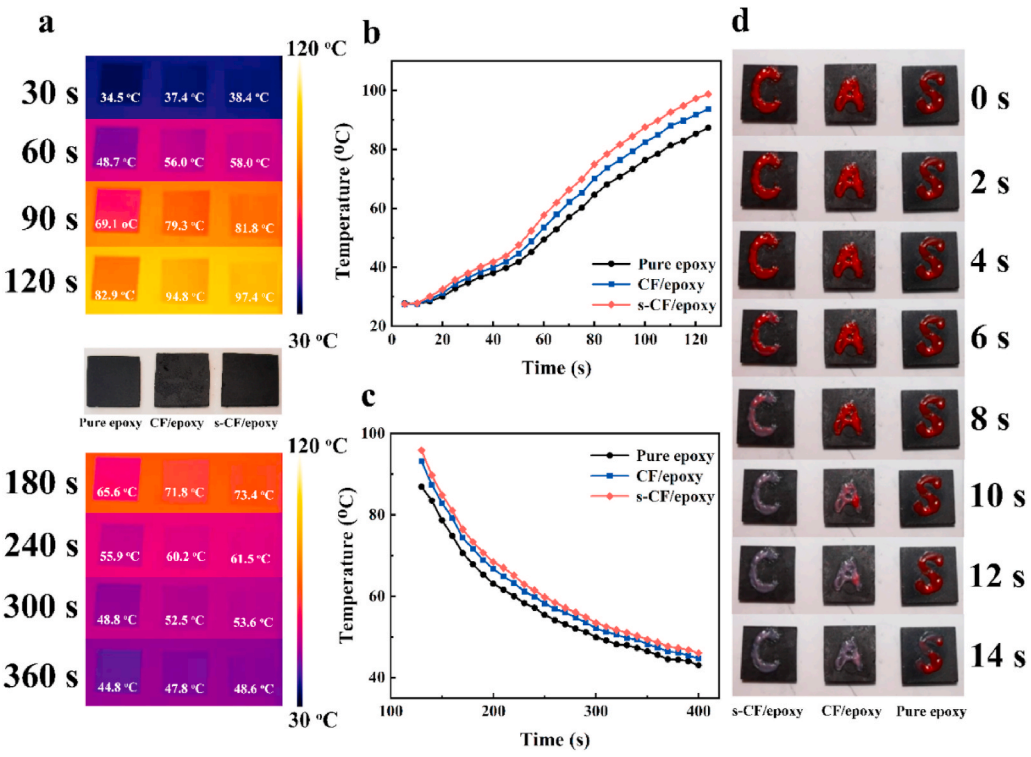

Fig. 5. Analysis of temperature field. **(a)** Infrared thermal image of s-CF/epoxy, CF/epoxy and pure epoxy at different moment during heating and cooling. **(b,c)** The temperature of samples during heating **(b)** and cooling**(c)**. **(d)**Schematic illustration of thermochromic display device with thermochromic ink pattern on different samples on the hotplate.

including various metal, carbon nanotubes, glass fiber, ceramic, and CF [22,23,39–60]. The thermal conductivity values, the resins used, and literature are listed in the supplementary material in Table S2. It should be noted that volume fractions are commonly reported as opposed to weight fractions. To allow for a direct comparison between different fillers, volume fractions have been converted to weight fraction. The original concentration data are listed in the Table S2. In Fig. 4(e), the best result for s-CF/epoxy is labeled with a red, hollow star. The result is competitive even compared with the use of metal fillers. In Fig. 4(f), the TCE of samples with highest thermal conductivity for a wide variety of fillers are calculated and compared. Since most polymer matrices are thermal insulating, TCE of the different fillers is consistent with their thermal conductivity.

To demonstrate the behavior of the thermal conductivity of these composites for different weight percentages of fill loading, samples are heated together on a hotplate. Fig. 5(a) shows the infrared images extracted during the heating process. During the heating sequence, infrared images are token every 30 s and during the cooling process, the time is extended to 60 s. A darker color represents a lower temperature whereas the lighter color represents higher temperatures. Clear to see is that the temperature of s-CF/epoxy rises faster than that of the CF/epoxy and epoxy samples. After 120 s, the heater is turned off and the samples reaches a peak temperature for the s-CF/epoxy, CF/epoxy and pure epoxy samples are 97.4, 94.8 and 82.9 °C, respectively. The temperature difference between the s-CF/epoxy, CF/epoxy and pure epoxy can be determined from both the infrared images and curing temperature presented in Fig. 5(b). During the cooling process, although the temperature of the s-CF/epoxy is always highest because of the initial temperature difference, the temperature difference between the samples rapidly decreases with time. After 360 s, the temperature of the s-CF/epoxy, CF/epoxy and epoxy samples are 48.6, 47.8 and 44.8 °C, respectively, which is markedly smaller than that at 120 s. The temperature during cooling process is record and presented in Fig. 5(c). These thermal conductive materials clearly have practical applications. We note a novel use of the composites as a rapid response material in temperature control. Here thermochromic ink which is red at room temperature and becomes white as temperature rises beyond 65 °C is panted on the top surface of samples heated by ceramic heater. It took the s-CF/epoxy 10 s to reach the temperature for the color transition whereas it took the CF/epoxy an additional 4 s to research the transition. The pure epoxy sample does not reach the transition temperature before during the observation period. This trend is consistent with the thermal conductivity test result, supporting our conclusion that the s-CF/epoxy possess an out-standing ability to transport heat.

4. Conclusion

In summary, we have fabricated a highly thermally conductive epoxy composite by stress induced orientation of CFs. Comparison with the existing composites using one-dimensional fillers, the s-CF/epoxy realized a high thermal conductivity of 32.6 W m^{-1} K^{-1} with a CF filler loading of 46 wt%. A new thermal conductivity enhancement record of 14,650% is reported. The main reason for this high value is that the orientation of CFs along the through-plane direction and a directly connected network between the CFs which builds an efficient heat path. Furthermore, we substantiate the orientation of CFs whose influence on thermal conductivity is demonstrated both by finite analysis and micro-CT statistics. As stress orientation is compatible with standard industrial processes, the proposed method has distinct advantages and a high potential in constructing filler frameworks to develop highly thermally conductive composites, which have broad applications electronics and beyond.

Declaration of competing interest

The authors declare that they have no known competing financial interests or personal relationships that could have appeared to influence the work reported in this paper.

Acknowledgement

The authors are grateful for the financial support by the National Natural Science Foundation of China (51573201), the National Key Research and Development Project (2017YFE0128600), NSFC-Zhejiang Joint Fund for the Integration of Industrialization and Informatization (U1709205), Public Welfare Project of Zhejiang Province (2016C31026), The Scientific Instrument Developing Project of the Chinese Academy of Sciences (YZ201640), the Strategic Priority Research Program of the Chinese Academy of Sciences (XDA22000000), and the Science and Technology Major Project of Ningbo (2016S1002 and 2016B10038). We also thank the Chinese Academy of Sciences for the Hundred Talents Program, the Chinese Central Government for the Thousand Young Talents Program, 3315 Program of Ningbo.

Appendix A. Supplementary data

Supplementary data to this article can be found online at https://doi.org/10.1016/j.compositesb.2020.108599.

References

[1] Yang X, Zhong X, Zhang J, Gu J. Intrinsic high thermal conductive liquid crystal epoxy film simultaneously combining with excellent intrinsic self-healing performance. J Mater Sci Technol 2021;68:209–15.
[2] Yang X, Zhu J, Yang D, Zhang J, Guo Y, Zhong X, et al. High-efficiency improvement of thermal conductivities for epoxy composites from synthesized liquid crystal epoxy followed by doping BN fillers. Compos B Eng 2020;185:107784.
[3] Kim S-H, Rhee KY, Park S-J. Amine-terminated chain-grafted nanodiamond/epoxy nanocomposites as interfacial materials: thermal conductivity and fracture resistance. Compos B Eng 2020;192:107983.
[4] Xiao C, Guo Y, Tang Y, Ding J, Zhang X, Zheng K, et al. Epoxy composite with significantly improved thermal conductivity by constructing a vertically aligned three-dimensional network of silicon carbide nanowires/boron nitride nanosheets. Compos B Eng 2020;187:107855.
[5] Verma R, Nagendra HN, Mahesh Kumar VB, Vivek GA, Kasthurirengan S, Shivaprakash NC, et al. Performance improvement of cryosorption pump by enhancing thermal conductivity of epoxy-aluminum composite. Compos B Eng 2019;176:107163.
[6] Yu C, Zhang J, Li Z, Tian W, Wang L, Luo J, et al. Enhanced through-plane thermal conductivity of boron nitride/epoxy composites. Compos Part A Appl Sci Manuf 2017;98:25–31.
[7] Guo Y, Ruan K, Shi X, Yang X, Gu J. Factors affecting thermal conductivities of the polymers and polymer composites: a review. Compos Sci Technol 2020;193:108134.
[8] Zhu Z, Li C, Songfeng E, Xie L, Yao Y. Enhanced thermal conductivity of polyurethane composites via engineering small/large sizes interconnected boron nitride nanosheets. Compos Sci Technol 2019;170:93–100.
[9] Ma T, Zhao Y, Ruan K, Liu X, Zhang J, Guo Y, et al. Highly thermal conductivities, excellent mechanical robustness and flexibility, and outstanding thermal stabilities of aramid nanofiber composite papers with nacre-mimetic layered structures. ACS Appl Mater Interfaces 2020;12(1):1677–86.
[10] Zhang J, Wang X, Yu C, Li Q, Li Z, Li C, et al. A facile method to prepare flexible boron nitride/poly(vinyl alcohol) composites with enhanced thermal conductivity. Compos Sci Technol 2017;149:41–7.
[11] Guan C, Qin Y, Bo w, Li L, Wang M, Lin C-T, et al. Highly thermally conductive polymer composites with barnacle-like nano-crystalline Diamond@Silicon carbide hybrid architecture. Compos B Eng 2020;198:108167.
[12] Li M, Wang M, Hou X, Zhan Z, Wang H, Fu H, et al. Highly thermal conductive and electrical insulating polymer composites with boron nitride. Compos B Eng 2020;184:107746.
[13] Guo S, Zheng R, Jiang J, Yu J, Dai K, Yan C. Enhanced thermal conductivity and retained electrical insulation of heat spreader by incorporating alumina-deposited graphene filler in nano-fibrillated cellulose. Compos B Eng 2019;178:107489.
[14] Yu S, Park K, Lee J-W, Hong SM, Park C, Han TH, et al. Enhanced thermal conductivity of epoxy/Cu-plated carbon fiber fabric composites. Macromol Res 2017;25(6):559–64.
[15] Bekyarova E, Thostenson E, Yu A, Kim H, Gao J, Tang J, et al. Multiscale carbon nanotube-carbon fiber reinforcement for advanced epoxy composites. Langmuir 2007;23(7):3970–4.
[16] Wang H, Li L, Chen Y, Li M, Fu H, Hou X, et al. Efficient thermal transport highway construction within epoxy matrix via hybrid carbon fibers and alumina particles. ACS Omega 2020;5(2):1170–7.
[17] Guo L, Zhang Z, Li M, Kang R, Chen Y, Song G, et al. Extremely high thermal conductivity of carbon fiber/epoxy with synergistic effect of MXenes by freeze-drying. Compos Commun 2020;19:134–41.
[18] Ruan K, Shi X, Guo Y, Gu J. Interfacial thermal resistance in thermally conductive polymer composites: a review. Compos Commun 2020;22:100518.
[19] Han Y, Shi X, Yang X, Guo Y, Zhang J, Kong J, et al. Enhanced thermal conductivities of epoxy nanocomposites via incorporating in-situ fabricated hetero-structured SiC-BNNS fillers. Compos Sci Technol 2020;187:107944.
[20] Yu W, Fu J, Chen L, Zong P, Yin J, Shang D, et al. Enhanced thermal conductive property of epoxy composites by low mass fraction of organic-inorganic multilayer covalently grafted carbon nanotubes. Compos Sci Technol 2016;125:90–9.
[21] Varshney V, Roy AK, Baur JW. Modeling the role of bulk and surface characteristics of carbon fiber on thermal conductance across the carbon-fiber/matrix interface. ACS Appl Mater Interfaces 2015;7(48):26674–83.
[22] Uetani K, Ata S, Tomonoh S, Yamada T, Yumura M, Hata K. Elastomeric thermal interface materials with high through-plane thermal conductivity from carbon fiber fillers vertically aligned by electrostatic flocking. Adv Mater 2014;26(33):5857–62.
[23] Ren L, Zhou X, Xue J, Song Z, Li B, Liu Q, et al. Thermal metamaterials with site-specific thermal properties fabricated by 3D magnetic printing. Adv Mater Technol 2019:1900296.
[24] Nakano Y, Matsuo M. Orientation behavior of carbon fiber axes in polymer solutions under magnetic field estimated in terms of orientation distribution function. J Mater Chem C 2008;112(40):15611–22.
[25] Yang XT, Fan SG, Li Y, Guo YQ, Li YG, Ruan KP, et al. Synchronously improved electromagnetic interference shielding and thermal conductivity for epoxy nanocomposites by constructing 3D copper nanowires/thermally annealed graphene aerogel framework. Compos Part A Appl Sci Manuf 2020;128:105670.
[26] Ma JK, Shang TY, Ren LL, Yao YM, Zhang T, Xie JQ, et al. Through-plane assembly of carbon fibers into 3D skeleton achieving enhanced thermal conductivity of a thermal interface material. Chem Eng J 2020;380:8.
[27] Hou X, Chen Y, Dai W, Wang Z, Li H, Lin C, et al. Highly thermal conductive polymer composites via constructing micro-phragmites communis structured carbon fibers. Chem Eng J 2019;375:121921.
[28] Zhang X, Zhang J, Li C, Wang J, Xia L, Xu F, et al. Endowing the high efficiency thermally conductive and electrically insulating composites with excellent antistatic property through selectively multilayered distribution of diverse functional fillers. Chem Eng J 2017;328:609–18.
[29] Zhang X, Zhang J, Xia L, Li C, Wang J, Xu F, et al. Simple and consecutive melt extrusion method to fabricate thermally conductive composites with highly oriented boron nitrides. ACS Appl Mater Interfaces 2017:22977–84.
[30] Zhang X, Zhang J, Zhang X, Li C, Wang J, Li H, et al. Toward high efficiency thermally conductive and electrically insulating pathways through uniformly dispersed and highly oriented graphites close-packed with SiC. Compos Sci Technol 2017;150(sep.29):217–26.
[31] Zhang X, Zhang J, Xia L, Wang J, Li C, Xu F, et al. Achieving high-efficiency and robust 3D thermally conductive while electrically insulating hybrid filler network with high orientation and ordered distribution. Chem Eng J 2018;334:247–56.
[32] Xu Z, Chen Y, Li W, Li J, Yu H, Liu L, et al. Preparation of boron nitride nanosheet-coated carbon fibres and their enhanced antioxidant and microwave-absorbing properties. RSC Adv 2018;8(32):17944–9.
[33] Malard L, Pimenta M, Dresselhaus G, Dresselhaus M. Raman spectroscopy in graphene. Phys Rep 2009;473(5–6):51–87.
[34] Agari Y, Ueda A, Nagai S. Thermal conductivity of a polyethylene filled with disoriented short-cut carbon fibers. J Appl Polym Sci 1991;43(6):1117–24.
[35] Chen J, Wang K, Zhao Y. Enhanced interfacial interactions of carbon fiber reinforced PEEK composites by regulating PEI and graphene oxide complex sizing at the interface. Compos Sci Technol 2018;154:175–86.
[36] Dong S, Gauvin R. Application of dynamic mechanical analysis for the study of the interfacial region in carbon fiber/epoxy composite materials. Polym Compos 1993;14(5):414–20.
[37] Ziegel K, Romanov A. Modulus reinforcement in elastomer composites. I. Inorganic fillers. J Appl Polym Sci 1973;17(4):1119–31.
[38] Ziegel KD. Role of the interface in mechanical energy dissipation of composites. J Colloid Interface Sci 1969;29(1):72–80.
[39] Xia C, Garcia AC, Shi SQ, Qiu Y, Warner N, Wu Y, et al. Hybrid boron nitride-natural fiber composites for enhanced thermal conductivity. Sci Rep 2016;6:34726.
[40] Wang Z, Liu J, Cheng Y, Chen S, Yang M, Huang J, et al. Alignment of boron nitride nanofibers in epoxy composite films for thermal conductivity and dielectric breakdown strength improvement. Nanomaterials 2018;8(4):242.
[41] Kusunose T, Yagi T, Firoz SH, Sekino T. Fabrication of epoxy/silicon nitride nanowire composites and evaluation of their thermal conductivity. J Mater Chem A 2013;1(10):3440–5.
[42] Kim SH, Heo Y-J, Park M, Min B-G, Rhee KY, Park S-J. Effect of hydrophilic graphite flake on thermal conductivity and fracture toughness of basalt fibers/epoxy composites. Compos B Eng 2018;153:9–16.
[43] Yuan L, Ma B, Zhu Q, Zhang X, Zhang H, Yu J. Preparation and properties of mullite-bonded porous fibrous mullite ceramics by an epoxy resin gel-casting process. Ceram Int 2017;43(7):5478–83.
[44] Rajadurai A. Thermo-mechanical characterization of siliconized E-glass fiber/hematite particles reinforced epoxy resin hybrid composite. Appl Surf Sci 2016;384:99–106.
[45] Zheng L-F, Wang L-N, Wang Z-Z, Wang L. Effects of γ-ray irradiation on the fatigue strength, thermal conductivities and thermal stabilities of the glass fibres/epoxy resins composites. Acta Metall Sin 2018;31(1):105–12.
[46] Choi JH, Song HJ, Jung J, Yu JW, You NH, Goh M. Effect of crosslink density on thermal conductivity of epoxy/carbon nanotube nanocomposites. J Appl Polym Sci 2017;134(4).
[47] Chen J, Yan L, Song W, Xu D. Thermal and electrical properties of carbon nanotube-based epoxy composite materials. Mater Res Express 2018;5(6):065051.

[48] Liu Z, Li H, Gu J, Wang D, Qu C. Performances of an epoxy-amine network after introducing the MWCNTs: rheology, thermal and electrical conductivity, mechanical properties. J Adhes Sci Technol 2019;33(4):382–94.
[49] Brown M, Jagannadham K. Thermal conductivity of MWNT-epoxy composites by transient thermoreflectance. J Electron Mater 2015;44(8):2624–30.
[50] Hong W-T, Tai N-H. Investigations on the thermal conductivity of composites reinforced with carbon nanotubes. Diam Relat Mater 2008;17(7–10):1577–81.
[51] Liao G, You Q, Xia H, Wang D. Preparation and properties of novel epoxy composites containing electrospun PA6/F-MWNTs fibers. Polym Eng Sci 2016;56 (11):1259–66.
[52] Huang H, Liu C, Wu Y, Fan S. Aligned carbon nanotube composite films for thermal management. Adv Mater 2005;17(13):1652–6.
[53] Fang Z, Li M, Wang S, Gu Y, Li Y, Zhang Z. Through-thickness thermal conductivity enhancement of carbon fiber composite laminate by filler network. Int J Heat Mass Tran 2019;137:1103–11.
[54] Noh YJ, Kim SY. Synergistic improvement of thermal conductivity in polymer composites filled with pitch based carbon fiber and graphene nanoplatelets. Polym Test 2015;45:132–8.
[55] Wei J, Liao M, Ma A, Chen Y, Duan Z, Hou X, et al. Enhanced thermal conductivity of polydimethylsiloxane composites with carbon fiber. Compos Commun 2020;17: 141–6.
[56] Xu J, Munari A, Dalton E, Mathewson A, Razeeb KM. Silver nanowire array-polymer composite as thermal interface material. J Appl Phys 2009;106(12): 124310.
[57] Li Z, Zhang L, Qi R, Xie F, Qi S. Improvement of the thermal transport performance of a poly(vinylidene fluoride) composite film including silver nanowire. J Appl Polym Sci 2016;133(25):43554.
[58] Balachander N, Seshadri I, Mehta RJ, Schadler LS, Borca-Tasciuc T, Keblinski P, et al. Nanowire-filled polymer composites with ultrahigh thermal conductivity. Appl Phys Lett 2013;102(9):093117.
[59] Seshadri I, Esquenazi GL, Borca-Tasciuc T, Keblinski P, Ramanath G. Multifold Increases in thermal conductivity of polymer nanocomposites through microwave welding of metal nanowire fillers. Adv Mater Interfaces 2015;2(15):1500186.
[60] Wang S, Cheng Y, Wang R, Sun J, Gao L. Highly thermal conductive copper nanowire composites with ultralow loading: toward applications as thermal interface materials. ACS Appl Mater Interfaces 2014;6(9):6481–6.